

# Supplementary Material:

## How Metallic are Noble-Metal Clusters? Static Screening and Polarizability in Quantum-Sized Silver and Gold Nanoparticles

Rajarshi Sinha-Roy,<sup>\*,†,‡,§</sup> Pablo García-González,<sup>‡,§</sup> and Hans-Christian Weissker<sup>\*,¶,§</sup>

<sup>†</sup>*Aix Marseille Univ, CNRS, CINAM, Marseille, France*

<sup>‡</sup>*Departamento de Física Teórica de la Materia Condensada and Condensed Matter Physics Center (IFIMAC), Universidad Autónoma de Madrid, E-28049 Madrid, Spain*

<sup>¶</sup>*Aix-Marseille University, CNRS, CINAM, Marseille, France.*

<sup>§</sup>*European Theoretical Spectroscopy Facility (ETSF)*

E-mail: sinharoy@cinam.univ-mrs.fr; weissker@cinam.univ-mrs.fr

# Static response of small Ag and Au shell structures

In Fig. S1 we compare the induced dipole moments of Ag and Au shell structures derived from the compact 309-atom icosahedra with those deriving from the 147- and 55-atom icosahedra. As indicated in the manuscript, the overall behavior for these smaller structures is the same.

One exception among these systems is the 147-derived 144-atom cluster. Here, one atom removed is not enough to obtain a clear result. To check the generality of the effects, we removed three atoms (the center atoms and the two adjacent atoms along the axis). This produced the effect that appears to be fully comparable to the results of 55 (one atom removed) and 309 (13 atoms removed.) However, as in addition to the creation of the cavity, in this case the spherical (or, in this case, icosahedral) symmetry is broken. Therefore, we do not insist on that system in the discussion in the main manuscript.

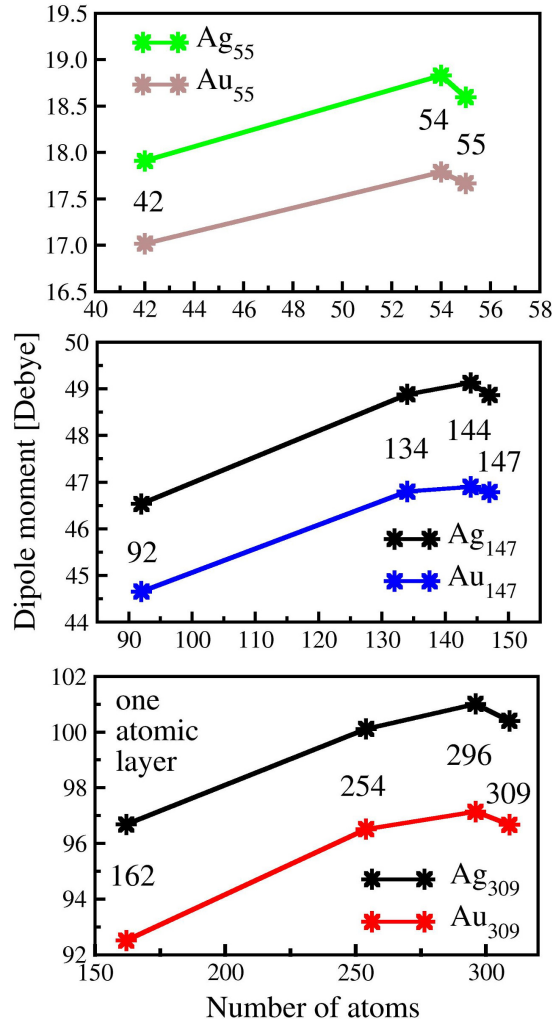


**Fig. S1.** Dipole moments of Ag and Au shell structures derived from different compact clusters: 55-atom icosahedra, and 147-atom icosahedra, and 309-atom icosahedra (the same as in Fig. 2 of the manuscript).

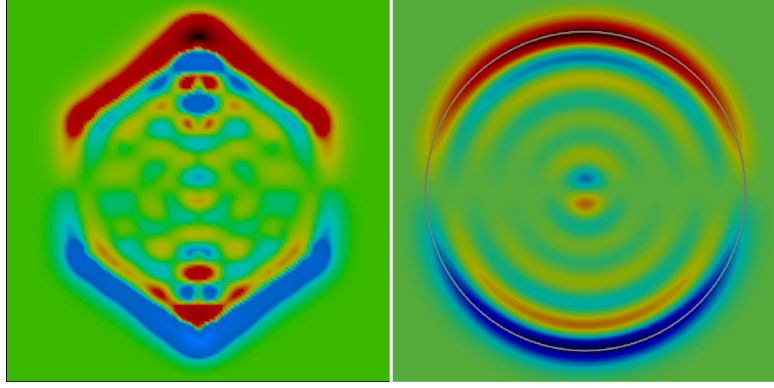


**Fig. S2.** Induced densities, comparing the 309-atom icosahedron of atomistic Na (LHS) with the 338-atom Na-jellium (RHS).

## Induced densities of atomistic and jellium structures

Aiming at assessing the validity of the jellium model to analyze the main trends found in atomistic structures, in Fig. S2 we compare the static induced densities for the atomistic icosahedral  $\text{Na}_{309}$  compact cluster and the spherical  $\text{Na}_{338}$  jellium compact structure. The overall similarity between both densities is evident, although the effects due to the icosahedral shape and the corrugation associated to the atomic structure can be observed for  $\text{Na}_{309}$ . In any case, it is noticeable that the number of Friedel-like oscillations is the same.

In Fig. S3, we show the induced densities for the *silver* and the jellium 162-atom shell structures. In addition to the differences between the icosahedral and spherical *shapes* as already described above, the difference due to the atom-centered polarization of silver *d*-electrons is clearly visible.

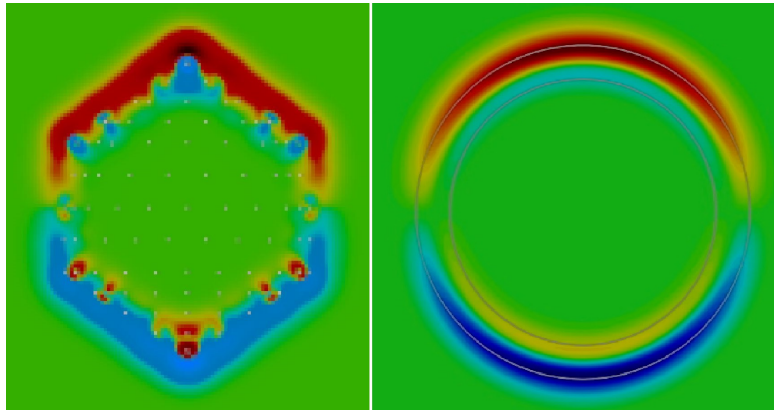


**Fig. S3.** Induced densities of the 162-atom shell structures of atomistic Ag (LHS) and Na-jellium (RHS).

# Screening of the E-field for jellium shell structures

For the jellium model with spherical symmetry, the induced electron density by an external homogeneous E-field  $\delta\mathbf{E}_{\text{ext}} = E_0\hat{\mathbf{z}}$  can be written as  $\delta n(\mathbf{r}) = \delta n_r(r) \cos(\theta)$ , where  $\theta$  is the azimuthal angle. The axial symmetry of the induced density makes solving the Poisson equation especially simple and, in particular, the induced E-field along the  $Z$  axis is given by

$$\delta\mathbf{E}_{\text{ind}}(0, 0, z) = \delta E_z(z)\hat{\mathbf{z}}, \text{ with } \delta E_z(z) = \frac{4\pi}{3} \left[ \int_{|z|}^{\infty} \delta n_r(u)du - \int_0^{|z|} \frac{2u^3}{|z|^3} \delta n_r(u)du \right]. \quad (1)$$

As a consequence, the total (external+induced) E-field at the center of the structure is

$$\delta\mathbf{E}_{\text{tot}}(\mathbf{0}) = \delta E_{\text{tot}}(\mathbf{0})\hat{\mathbf{z}}, \text{ with } \delta E_{\text{tot}}(\mathbf{0}) = E_0 + \frac{4\pi}{3} \int_0^{\infty} \delta n_r(u)du, \quad (2)$$

and the induced dipole moment is

$$\mathcal{P}_z\hat{\mathbf{z}} = \lim_{z \rightarrow \infty} \frac{z^3 \delta\mathbf{E}_{\text{ind}}(0, 0, z)}{2} = -\frac{4\pi}{3} \int_0^{\infty} u^3 \delta n_r(u)du \hat{\mathbf{z}}. \quad (3)$$

Thus, the function  $\delta E_z(z)$  provides direct information about the screening of the external E-field. If the system was a perfect metal,  $E_0 + \delta E_z(z) = 0$  within the structure.

In Fig. S4 we depict the dimensionless function  $[E_0 + \delta E_z(z)]/E_0$  for the Na-jellium shell structures built from the compact Na<sub>338</sub> jellium cluster and, for completeness, the contour plots of the induced charges. For the compact Na<sub>338</sub>, the induced density  $\delta n(\mathbf{r})$  spreads over the whole cluster. As a consequence, the total E-field is not constant within the cluster but oscillates around zero following the Friedel-like oscillations of the induced density. However, if we evaluate the average of  $\delta E_z(z)$  over  $0 < z < 0.61$  nm, which is the interval that corresponds to the cage of the three-layer shell structure Na<sub>314</sub>, we get  $\langle \delta E_z \rangle = -0.998E_0$ . We can thus affirm that, on average, the external E-field is practically screened around the center of the compact cluster up to a marginal amount of 0.2%.

On the other hand, for the three shell structures (Na<sub>314</sub>, Na<sub>262</sub>, and Na<sub>162</sub>) there is no induced density at the center of the system. Therefore, we can measure directly the efficiency of the screening from the value of the  $z$ -coordinate of the total E-field at the center of the system,  $\delta E_{\text{tot}}(\mathbf{0})$ . For the one-layer shell structure,  $\delta E_{\text{tot}}(\mathbf{0}) \simeq 0.05E_0$ , which means that a single atomic layer is able to screen 95% of the external E-field even in nanometric structures. For the two-layer structure, 97.5% of the external field are screened and, finally, for the three-layer structure, there is a slight *anti-screening* that produces an internal field of about -1% of the external field.

By comparing Eq. (2) and (3) we observe that the values of the induced dipole moment,  $\mathcal{P}_z$ , and the total E-field at the center of the system,  $\delta E_{\text{tot}}(\mathbf{0})$ , are correlated through the local induced density  $\delta n_r(r)$ . Since both the induced density and the E-field are practically the same for all the structures if  $r > r_c$ , where  $r_c \simeq 1.4$  nm, we may attribute the small changes on  $\mathcal{P}_z$  and  $\delta E_{\text{tot}}(\mathbf{0})$  to the different values of the induced density for  $r < r_c$ . Then, it is expected that the induced dipole moment and the screening will follow similar trends when varying the number of layers. This is indeed the case. We have seen that the screening is almost perfect for the compact Na<sub>338</sub> cluster. Therefore, the slightly greater polarizability of the three-layer Na<sub>314</sub> structure is consistent with the

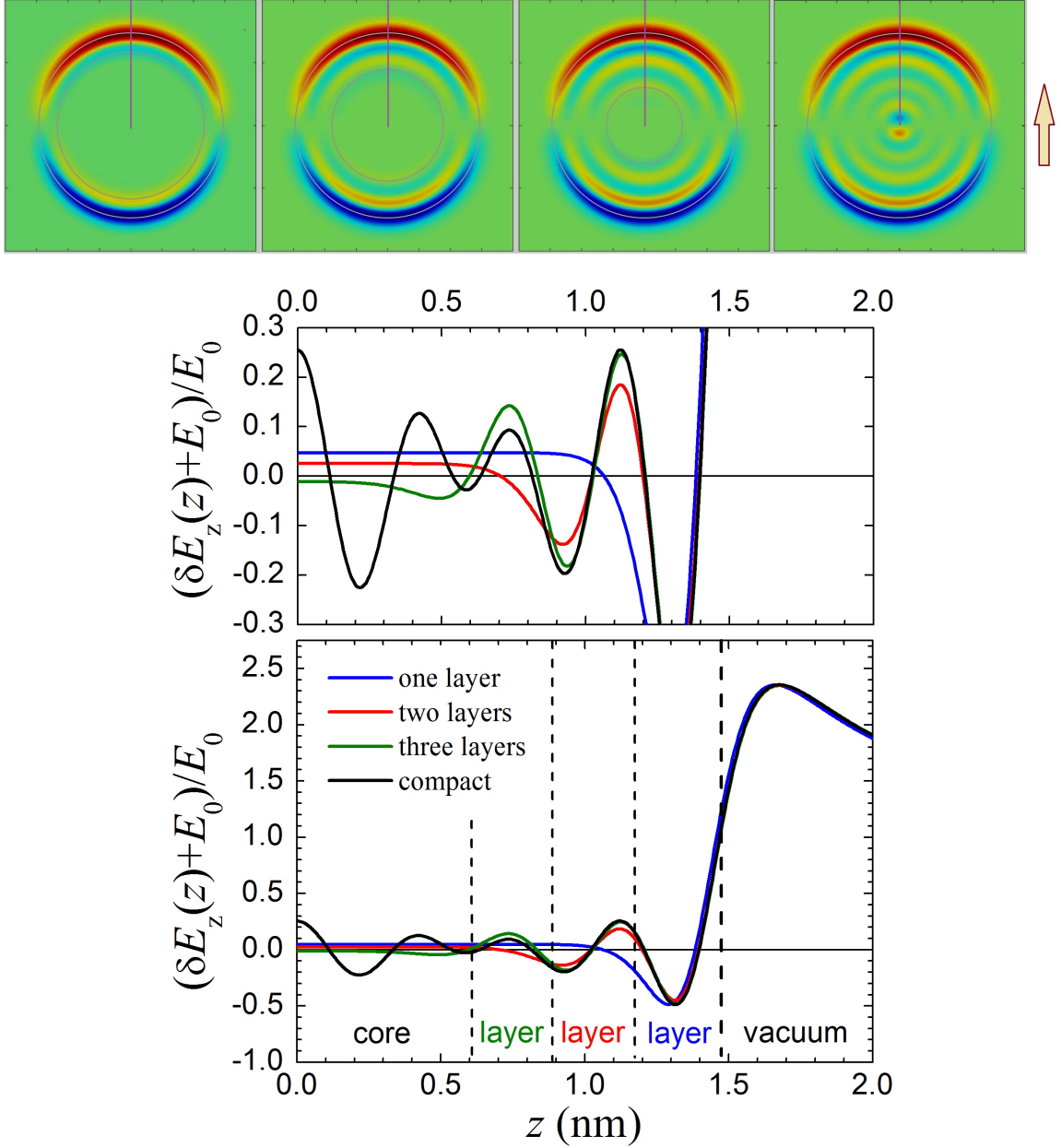


**Fig. S4.** Top panels: contour plots of the induced charge densities (red: positive, blue: negative), comparing the 338-atom Na-jellium cluster (last panel) with its shells (162, 262, and 314 “atoms”). Lower panels: total (induced + external) E-field along the direction of the incident E-field. Note that, as can be seen in more detail in the middle panel, the total E-field is constant and very small around the center of the system for the three shell structures.

above-mentioned small overscreening of the E-field. For the two- and one-layer structures ( $\text{Na}_{262}$  and  $\text{Na}_{162}$ ) the induced dipole moment is smaller than that of the compact cluster, and this is reflected by the respective amounts of screening (97.5% and 95%, respectively).